IJP: Drugs and Drug Resistance 9 (2019) 59–71

Contents lists available at ScienceDirect

IJP: Drugs and Drug Resistance

journal homepage: www.elsevier.com/locate/ijpddr

Tetrahydroquinoxalines induce a lethal evisceration phenotype in *Haemonchus contortus* in vitro

Yaqing Jiao[a], Sarah Preston[a,b], Jose F. Garcia-Bustos[a], Jonathan B. Baell[c,***], Sabatino Ventura[c], Thuy Le[c], Nicole McNamara[c], Nghi Nguyen[c], Antony Botteon[c], Cameron Skinner[d,e], Jill Danne[d,e], Sarah Ellis[d,e], Anson V. Koehler[a], Tao Wang[a], Bill C.H. Chang[a,f], Andreas Hofmann[a,g], Abdul Jabbar[a,**], Robin B. Gasser[a,*]

[a] Faculty of Veterinary and Agricultural Sciences, The University of Melbourne, Parkville, Victoria, Australia
[b] Faculty of Science and Technology, Federation University, Ballarat, Victoria, Australia
[c] Medicinal Chemistry, Monash Institute of Pharmaceutical Sciences, Monash University, Parkville, Victoria, Australia
[d] Centre for Advanced Histology and Microscopy, Peter MacCallum Cancer Centre, Parkville, Victoria, Australia
[e] Sir Peter MacCallum Department of Oncology, The University of Melbourne, Parkville, Victoria, Australia
[f] Yourgene Bioscience, Taipei, Taiwan
[g] Griffith Institute for Drug Discovery, Griffith University, Nathan, Queensland, Australia

ARTICLE INFO

Keywords:
Quinoxalines
Whole-organism screening
Evisceration (Evi) phenotype
Haemonchus
Moulting
Anthelmintic

ABSTRACT

In the present study, the anthelmintic activity of a human tyrosine kinase inhibitor, AG-1295, and 14 related tetrahydroquinoxaline analogues against *Haemonchus contortus* was explored. These compounds were screened against parasitic larvae - exsheathed third-stage (xL3) and fourth-stage (L4) - using a whole-organism screening assay. All compounds were shown to have inhibitory effects on larval motility, development and growth, and induced evisceration through the excretory pore in xL3s. The estimated IC_{50} values ranged from 3.5 to 52.0 μM for inhibition of larval motility or development. Cytotoxicity IC_{50} against human MCF10A cells was generally higher than 50 μM. Microscopic studies revealed that this eviscerated (Evi) phenotype occurs rapidly (< 20 min) and relates to a protrusion of internal tissues and organs (evisceration) through the excretory pore in xL3s; severe pathological damage in L4s as well as a suppression of larval growth in both stages were also observed. Using a relatively low concentration (12.5 μM) of compound m10, it was established that the inhibitor has to be present for a relatively short time (between 30 h and 42 h) during in vitro development from xL3 to L4, to induce the Evi phenotype. Increasing external osmotic pressure prevented evisceration and moulting, and xL3s remained unaffected by the test compound. These results point to a mode of action involving a dysregulation of morphogenetic processes during a critical time-frame, in agreement with the expected behaviour of a tyrosine kinase inhibitor, and suggest potential for development of this compound class as nematocidal drugs.

1. Introduction

Parasitic worms cause substantial morbidity and mortality in humans and animals, and major losses to food production globally (cf. Roeber et al., 2013; Hotez et al., 2014). In particular, some parasitic roundworms (nematodes) of the order Strongylida, also called strongylids, or bursate nematodes, cause some of the most important gastrointestinal diseases of livestock worldwide, affecting hundreds of millions of animals (including sheep, goats, cattle and/or pigs), with economic losses estimated at tens of billions of dollars per annum (Roeber et al., 2013; Thamsborg et al., 2013; Lane et al., 2015). These pathogens can cause gastroenteritis, anaemia and/or associated complications (depending on species), and death in severely affected animals, and many of them cause marked productivity losses through subclinical infections. Bursate nematodes are transmitted orally from contaminated pastures to the host through a direct life cycle (Beveridge and Emery, 2014): eggs are excreted in host faeces; the first-stage larvae (L1s) develop inside the egg, usually hatch within 1 day at

* Corresponding author.
** Corresponding author.
*** Corresponding author.
E-mail addresses: jonathan.baell@monash.edu (J.B. Baell), jabbara@unimelb.edu.au (A. Jabbar), robinbg@unimelb.edu.au (R.B. Gasser).

https://doi.org/10.1016/j.ijpddr.2018.12.007
Received 10 October 2018; Received in revised form 11 December 2018; Accepted 29 December 2018
Available online 30 December 2018

environmental temperatures of ≥10 °C and then develop to the second- and third-stage larvae (L2s and L3s) in about one week; the infective L3s are then ingested by the host, exsheath (xL3) and develop through fourth-stage larvae (L4) to dioecious adults (often within 3–4 weeks) in the gastrointestinal tract of the animal.

Currently, the control of these nematodes relies largely on the use of a limited number of anti-parasitic drug classes. However, drug resistance is now widespread (Kotze and Prichard, 2016), and no vaccines are available for the vast majority of these worms (Hewitson and Maizels, 2014), such that the development of new drugs is crucial to ensure sustained and effective control into the future. Although the development of monepantel (Kaminsky et al., 2008; Prichard and Geary, 2008) and derquantel (Little et al., 2011) has introduced novel classes of nematocides, success in discovering new anthelmintic drugs has been limited.

We have been focusing on identifying synthetic chemical entities with nematocidal or nematostatic activity (Preston et al., 2016b, 2017; Jiao et al., 2017a, 2017b), working toward the optimisation of their potency and selectivity. Recently, we obtained a collection of compounds ('Stasis Box') from Medicines for Malaria Venture (MMV); this collection contains 400 compounds which were under pharmaceutical development, and about which there is published information in the scientific literature or patents. Utilizing a whole-worm motility screening assay (Preston et al., 2015), we identified in the 'Stasis Box' a platelet-derived growth factor (PDGF) receptor kinase inhibitor (Kovalenko et al., 1994, 1997; Gazit et al., 1996) called AG-1295 (6,7-dimethyl-2-phenylquinoxaline), with relatively potent anthelmintic activity against *H. contortus* in vitro (Jiao et al., 2017a). Dose-response evaluations showed that AG-1295 inhibits the motility of exsheathed third-stage larvae (xL3s) and the development of fourth-stage larvae (L4s), with half maximum inhibitory concentration (IC_{50}) values of 9.9 ± 1.9 μM and 7.8 ± 0.9 μM, respectively (Jiao et al., 2017a). Moreover, AG-1295 was not toxic (IC_{50} > 100 μM) to normal human breast epithelial (MCF10A) cells when tested in vitro (Jiao et al., 2017a).

Interestingly, AG-1295 had been under development as a medicine for restenosis treatment (Levitzki, 2013). This kinase inhibitor has been reported to (i) attenuate porcine and human smooth muscle cell growth in vitro (Banai et al., 1998), (ii) block the proliferation of rat hepatic stellate cells in vitro (Iwamoto et al., 2000) and (iii) inhibit aortic allograft vasculopathy in rats (Karck et al., 2002). However, currently nothing is known about how AG-1295 affects or acts on *H. contortus* or any other nematode. Considering that AG-1295 can be classified as drug-like (Gazit et al., 1996), has suitable pharmacokinetic properties (Banai et al., 1998; Levitzki, 2001, 2010) and elicits dramatic effects on both motility and development of *H. contortus* in vitro (Jiao et al., 2017a), this compound and/or one or more analogues thereof might have potential for being repurposed as anthelmintics. In the present study, we extend previous work (Jiao et al., 2017a) to (i) explore the anthelmintic activities of 14 AG-1295 analogues (tetrahydroquinoxalines) on motility and development of larval stages of *H. contortus* in vitro, (ii) start investigating their mode of action by qualitatively and quantitatively assessing the morphological alterations that occur in larval stages of *H. contortus* following exposure to these analogues in vitro, and (iii) discuss how this worm is affected by representative compounds.

2. Materials and methods

2.1. Procurement of H. contortus

Haemonchus contortus (Haecon-5 strain; partially resistant to benzimidazoles) was maintained in Merino sheep in approved facilities in The University of Melbourne with institutional animal ethics approval (permit no. 1413429). Larval stages of *H. contortus* were produced as described previously (Preston et al., 2015). In brief, faeces were collected from infected sheep four weeks following inoculation and were then incubated at 27 °C for one week. Then, L3s were isolated from faeces and sieved through two layers of nylon mesh (pore size: 20 μm; Rowe Scientific, Australia). Exsheathed L3s (xL3s) were produced by incubating L3s in 0.15% (v/v) sodium hypochlorite (NaClO) at 37 °C for 20 min, and immediately washed five-times in sterile physiological saline by centrifugation (1700 × *g*, 5 min). The xL3s were resuspended in LB* [10 g of tryptone (cat. no. LP0042; Oxoid, England), 5 g of yeast extract (cat. no. LP0021; Oxoid, England) and 5 g of NaCl (cat. no. 1064045000; Merck, Denmark) in 1 l of reverse-osmosis deionized water; supplemented with 100 IU/ml of penicillin, 100 μg/ml of streptomycin and 0.25 μg/ml of amphotericin (antibiotic-antimycotic; cat. no. 15240062; Gibco, USA)]. L4s were produced by incubating xL3s in LB* at 38 °C and 10% (v/v) CO_2 for 7 days; larvae were not used unless ≥ 80% of xL3s developed to L4s - identified based on the appearance of a mouth and pharynx (Veglia, 1916; Sommerville, 1966).

2.2. AG-1295 analogues

A total of 14 tetrahydroquinoxaline compounds whose structures are closely related to AG-1295 were made in the laboratories of two co-authors (JBB and SV) (Supplementary file 1). All compounds were synthesized as arylated 5,6,7,8- tetrahydroquinoxaline *N*-oxide intermediates using palladium catalysis, and the *N*-oxide moiety was reduced to yield the final structures (Supplementary file 1). AG-1295 was purchased from a commercial company (IUPAC name: 6,7-dimethyl-2-phenylquinoxaline, cat. no. A425200, 99.9% purity, Toronto Research Chemicals, Canada).

2.3. Compound screening

Compounds were screened against xL3s of *H. contortus* using an established approach (Preston et al., 2016a). In brief, compounds were individually dissolved in dimethyl sulfoxide (DMSO, Ajax Finechem, Australia) to a stock concentration of 20 mM. To test their activity against *H. contortus*, individual compounds were diluted in LB* to the final concentration of 100 μM. All compounds were tested in triplicate; a commercial anthelmintic, monepantel (Zolvix, Elanco Animal Health, Switzerland) was used as a positive control (in triplicate), and LB* + 0.5% DMSO was used as a negative control (in sextuplicate). All compounds were tested using in a 96-well plate (Corning 3596; Life Sciences, USA) with 300 xL3s per well for 72 h at 38 °C and 10% (v/v) CO_2. Following incubation, worms were agitated using an orbital shaker at 37 °C for 20 min, and 5-s video recordings were taken of individual wells. Each video capture of each well was processed using a custom macro in the program Image J (1.47v, imagej.nih.gov/ij); larval motility in each well was expressed as a motility index (Mi), calculated as described previously (Preston et al., 2015). A compound was identified as active against *H. contortus* ('hit') if it reproducibly reduced the Mi value of xL3s by ≥ 70%, or if a phenotype was observed that differed from wildtype xL3 (i.e. LB* + 0.5% DMSO control).

2.4. Dose-response assessments of active compounds on xL3 and L4 motility, and L4 development

Active compounds were tested against *H. contortus* larvae at a range of concentrations to determine IC_{50} values, as described earlier (Preston et al., 2015). Stocks of individual compounds (20 mM) were diluted in LB* (50 μl) to 200 μM, and then serially titrated (in two-fold steps) across a 96-well flat bottom plate. Subsequently, 300 worms (either xL3s or L4s) in 50 μl of LB* were added to individual wells, and the plates were incubated in a water-jacketed CO_2 incubator at 38 °C and 10% (v/v) CO_2. After 24 h, 48 h and 72 h of incubation, worm motility index (Mi) values were measured and processed to generate an 18-point dose-response curve using GraphPad Prism (v.7) software. Following

motility measurement, the xL3 plates were re-incubated for four more days to assess the L4 development. IC_{50} values for each dose-response curve (xL3 motility, L4 motility and L4 development) were calculated by fitting a variable slope four-parameter equation, constraining the top value to 100%. Each assay was repeated at least two times in triplicate on different days.

2.5. Assessment of cytotoxicity

A 'normal' human breast epithelial cell line (MCF10A) was used to test the cytotoxic activity of compounds (Jiao et al., 2017a). In brief, using a 384-well flat bottom, black-walled plate (Corning, USA), 700 MCF10A cells in 40 µl DMEM-F12 [100 ng/ml cholera toxin (Sigma, Australia), 20 ng/ml human epidermal growth factor (EGF, Life Technologies, Australia), 10 µg/ml insulin (human; Novo Nordisk Pharmaceuticals Pty Ltd, Australia), 5% horse serum (Life Technologies, Australia) and 0.5 µg/ml hydrocortisone (Sigma, Australia)], were dispensed into wells using a liquid handling dispenser (BioTek, Vermont, USA). Plates were incubated at 37 °C and 5% (v/v) CO_2 for 24 h. Meanwhile, test compounds were diluted in the cell growth media from 250 µM to 15.6 µM in a two-fold serial way using an automated liquid handling robot (SciClone ALH3000 Lab Automation Liquid Handler, Caliper Lifesciences, USA). The diluted compounds (10 µl) were then added to cultured cells, with doxorubicin as a positive control and DMEM-F12 + 0.5% DMSO as a negative control. Following an incubation for 48 h, cells were fixed and stained with 4',6-diamidino-2-phenylindole (DAPI; 1:1000). Subsequently, cell nuclei present in each well were quantified using a high content imager (Cellomics Cell Insight Personal Cell Imager, Thermofisher Scientific, USA) at 10-times magnification (with a fixed exposure time of 0.12 s) and the Target Activation BioApplication within the Cellomics software. IC_{50} values for inhibition of MCF10A cell proliferation were calculated from dose-response curves, using a variable slope four-parameter equation in GraphPad Prism. Each assay was repeated two times in quadruplicate on different days. The selectivity indices (Si) of hit compounds were then calculated using the formula: Si = IC_{50} for MCF10A cells/IC_{50} for *H. contortus*.

2.6. Morphological examination of the eviscerated (Evi) phenotype induced by incubation with individual test compounds

Light microscopy was used to examine morphological alteration(s) in larvae caused by test compounds after 7 days. At each compound concentration tested, 30 larvae (fixed with 1% iodine) were classified as either 'normal xL3s', 'eviscerated xL3s' or 'L4s', using a light microscope (DP26 camera, Olympus, USA). The concentration at which each test compound induced maximum numbers of eviscerated larvae was recorded. Compounds were also tested for their ability to inhibit larval growth by measuring worm length and width microscopically (20-times magnification), using a corresponding concentration of DMSO as a negative control. For each treatment, the mean length and width of ≥30 larvae ± standard error of the mean were calculated, and a one-way ANOVA with Tukey's test was used to measure the statistical differences between different treatments. This assay was repeated two times on different days.

2.7. Scanning electron microscopy (SEM)

Larvae were also examined by SEM. Briefly, in a 96-well flat bottom plate, 300 worms (xL3s or L4s) in 50 µl of LB* were exposed to the concentration of test compound that induced the greatest number of larvae with an Evi phenotype, with a corresponding concentration of DMSO as a negative control (in sextuplicate). Subsequently, the plate was incubated at 38 °C and 10% (v/v) CO_2 for 72 h. For each treatment, worms were then pooled together and washed three times in 0.9% saline by centrifugation at 9000 × *g*. For SEM analysis, worms were fixed in 2.5% glutaraldehyde and 2% paraformaldehyde for 2 h, rinsed three times in 0.1 M sodium cacodylate trihydrate for 10 min, and then post-fixed in 1% osmium tetroxide at room temperature for 2 h. Fixed worms were rinsed again three times in distilled water for 15 min. Following fixation, 200 µl of concentrated worms were incubated on poly-L-lysine coated glass coverslips; the slips were pre-prepared by immersing them in poly-L-lysine solution for 10 min, drying in an oven at 60 °C for 10 min, immersing again in poly-L-lysine solution for 10 min and then drying them at room temperature. The coverslips with adhered nematodes were dehydrated in a graded ethanol series (30%, 50%, 70%, 90% and 100%) for 17 min, dried in a critical point dryer (EM CPD300, Leica, Wetzlar, Germany), mounted on to aluminium stubs (25 mm) with double-sided carbon tabs and then coated with gold. Worms were imaged using a JEOL JCM-6000 Plus NeoScope scanning electron microscope (JEOL, Tokyo, Japan); at least six worms were examined for each treatment group.

2.8. Transmission electron microscopy (TEM)

Individual xL3s and L4s were fixed in 2.5% paraformaldehyde and 2% glutaraldehyde buffered with 0.1 M sodium cacodylate trihydrate (pH 7.2) and sliced into three even (anterior, mid and posterior) body portions (cf. Kovacs, 2015). After 2 h of primary fixation, worm portions were rinsed three times in 0.1 M sodium cacodylate trihydrate for 2 h, and then post-fixed in 1% osmium tetroxide and 1.5% potassium ferrocyanide in the dark for 2 h. Fixed worm portions were rinsed again three times in 0.1 M sodium cacodylate trihydrate for 2 h and then embedded in 1.5% agar. The agar blocks containing worm portions were washed two times in distilled water for 2 h and dehydrated in a graded ethanol series (50%, 70%, 90%, 95% and 100%) for 2 h on a platform rocker, rinsed two times in 100% acetone for 45 min, rocking, and then embedded in Spurrs resin. Ultrathin sections were cut with an EM UC7 ultramicrotome (Leica Microsystems GmbH, Wetzlar, Germany) and contrasted with lead citrate and aqueous uranyl acetate. Sections were imaged using a transmission electron microscope (JEOL 1011, Tokyo, Japan) with a MegaView III CCD cooled digital camera (Soft Imaging Systems, Münster, Germany).

2.9. Evaluation of the dynamics of the compound-induced Evi phenotype in xL3s

To determine the kinetics of the anterior protrusion and evisceration in xL3s, a time course experiment was performed using the compound concentration that caused maximum numbers of worms with the Evi phenotype. At various time-points (every 6 h for the first 4 days and then every 24 h for the next 3 days) after treatment, aliquots (50 µl) of 150 larvae were fixed in 1% iodine, and 30 worms from each aliquot were scored as either 'normal xL3s', 'eviscerated xL3s' or 'L4s' under a compound microscope using 100-times magnification. For each time point, the percentage of larvae in each category was calculated, and a two-way ANOVA with Tukey's test was used to calculate statistical differences between groups. This assay was repeated at least two times in triplicate on different days.

2.10. Assessment of the reversibility of effect of test compounds on xL3s

To determine whether the effect of test compounds on xL3 was reversible, a previously published method was used (Kumarasingha et al., 2016). In brief, xL3s were exposed for 18 h, 24 h, 27 h, 30 h, 36 h and 48 h to 12.5 µM of test compound in triplicate in 96-well plates. Following exposure, at each of these time points, compounds were removed by washing larvae three times in 0.9% saline, 100 µl of LB* were added to individual wells, and the plate was then re-incubated in a water-jacketed CO_2 incubator at 38 °C and 10% (v/v) CO_2. After 72 h, the percentages of the eviscerated xL3s and the L4s were calculated. Controls included xL3s continually incubated with 12.5 µM of test

compound (in triplicate) for 72 h and xL3s incubated in LB* alone. This assay was repeated two times in duplicate on different days. Differences in percentage of eviscerated xL3s between treatments were evaluated using a one-way ANOVA with Tukey's test.

Subsequently, xL3s were cultured first in LB*, and test compound (to 12.5 μM) was added to individual wells at two different time-points (39 h and 42 h). Again, worms were scored microscopically at 72 h. A matched compound concentration, added at 0 h, was used as a positive control, and the corresponding concentration of DMSO was used as a negative control. This assay was repeated two times in duplicate on different days. A two-way ANOVA with Tukey's test was used to measure statistical differences between treatments in the percentages of eviscerated xL3s and developed L4s.

2.11. Influence of external osmotic pressure on compound-induced Evi phenotype in xL3s

To examine whether an osmotic pressure gradient was involved in the induction of the Evi phenotype in xL3s, compound-treated and untreated xL3s were cultured in the presence of increasing concentrations of sorbitol (0 M–1.0 M in 0.1 M intervals) in LB*. After 72 h of incubation at 38 °C and 10% (v/v) CO_2, the percentages of the eviscerated xL3s and the developed L4s were calculated for each sorbitol concentration. This assay was repeated two times in duplicate on different days.

Since hypertonic sorbitol itself was observed to inhibit xL3 moulting, the reversibility of this effect was also tested. To do this, xL3s cultured in the presence of 0.6 M sorbitol for 48 h were washed three times in 0.9% saline and then placed in fresh LB*, and worms were examined microscopically after 7 days in culture. The controls included xL3s continually incubated in 0.6 M sorbitol (in triplicate) for 7 days, and xL3s incubated in LB* alone for the same period.

The reversibility of compound effect on xL3s, while xL3 moulting was inhibited by hypertonic sorbitol, was also assessed. Thus, xL3s were exposed to 12.5 μM of test compound in the presence of 0.6 M sorbitol, washed at 48 h and examined microscopically after 7 days in culture. Unwashed xL3s exposed to 12.5 μM of test compound in the presence of 0.6 M sorbitol for 7 days were used as a control for complete osmotic protection, and xL3s exposed to a matching concentration of test compound in LB* represented the control for a lack of osmotic protection. A two-way ANOVA with Tukey's test was used to calculate statistical differences between treatment groups. This assay was repeated two times in duplicate on different days.

3. Results

3.1. Inhibitory effects of AG-1295 analogues on xL3 motility, L4 motility and L4 development

Fourteen AG-1295 analogues (Supplementary file 1) and AG-1295 itself (reference compound; Fig. 1A) were tested against *H. contortus* in the established whole-worm screening assay. The reduction of Mi values of xL3s treated for 72 h with 100 μM of each of the analogues ranged from 11% to 65%, and an Evi phenotype was observed (Fig. 1B and C). At this concentration and after 7 days, L4 development was fully inhibited (100%) by all compounds, except m13 (48.6%).

Dose-response evaluations of xL3 motility established the potencies of individual compounds at 24 h, 48 h and 72 h. Four compounds (m6, m7, m13 and m14) gave full dose-response curves, with IC_{50} values ranging from 9.8 μM to 50.1 μM at 72 h (Table 1; Fig. 2A).

Ten analogues (m1, m2, m3, m4, m6, m8, m9, m10, m11 and m12) displayed an inhibitory effect on L4 motility, with IC_{50} values (at 72 h) ranging from 6.9 ± 2.8 μM to ~52.0 μM (Table 1; Fig. 2B). Compound m10 was most potent, with an IC_{50} value of 6.9 ± 2.8 μM. At shorter incubation times, individual compounds tended to be less potent at inhibiting L4 motility (Table 1; Fig. 2B).

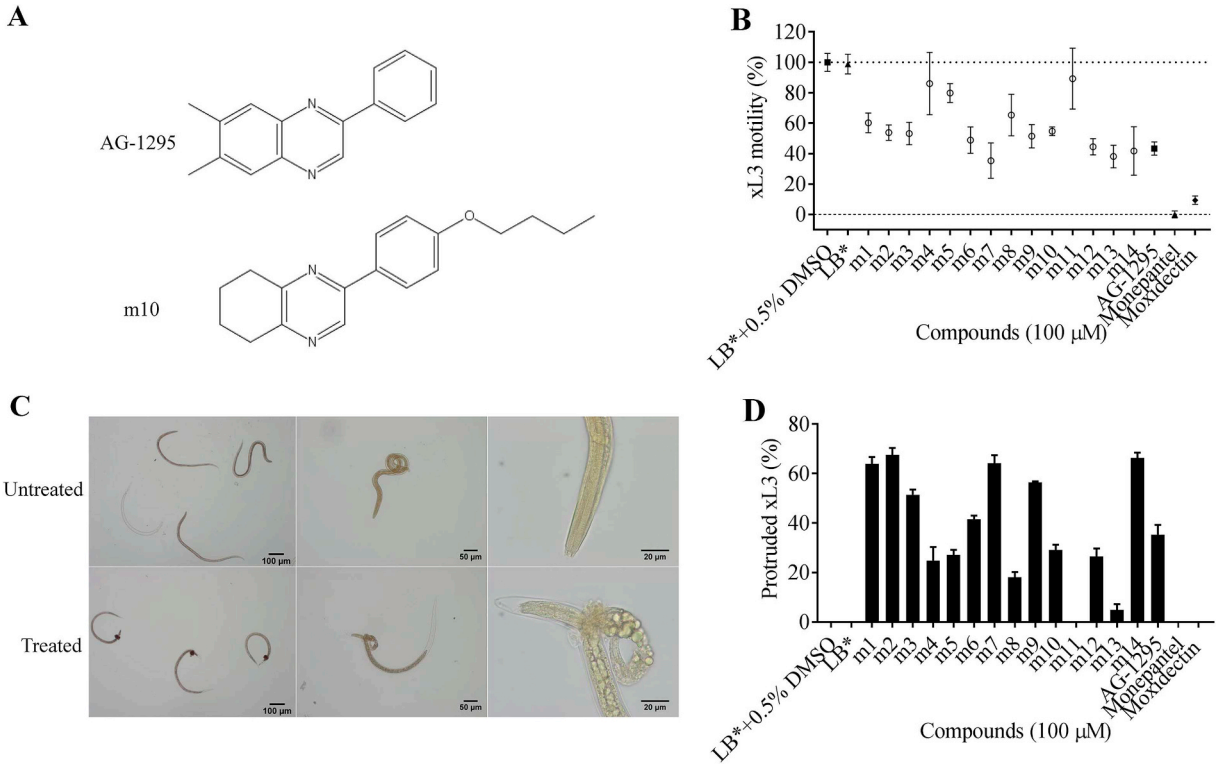

Fig. 1. Screening of 14 tetrahydroquinoxalines against exsheathed third-stage larvae (xL3s) of *Haemonchus contortus*. Panel A: Chemical structures of AG-1295 and one representative tetrahydroquinoxaline analogue m10. Panel B: Primary screen for inhibition of xL3 motility after 72 h of compound treatment. Panel C: The compound-induced Evi phenotype in xL3s after 7 days of compound treatment. Panel D: Percentages of eviscerated xL3s induced by individual compounds. Positive controls were monepantel and moxidectin, and negative controls were corresponding concentrations of dimethyl sulfoxide (DMSO).

Table 1
In vitro activities of 14 tetrahydroquinoxaline compounds against *Haemonchus contortus*. Half maximum inhibitory concentration (IC_{50}) values of test compounds on the motility of exsheathed third-stage (xL3) and fourth-stage (L4) larvae after 24 h, 48 h and 72 h of exposure, and on L4 development after 7 days of exposure, in comparison with values for monepantel and AG-1295 (± standard error of the mean). Each assay was repeated at least two times in triplicate on different days.

Compound	Half maximum inhibitory concentration (IC_{50} μM)						
	xL3 motility			L4 motility			L4 development
	24 h	48 h	72 h	24 h	48 h	72 h	7 days
m1	–	–	–	–	52.8 ± 3.8	34.1 ± 9.1	18.0 ± 2.0
m2	–	–	–	–	–	81.2 ± 16.6	–
m3	–	–	–	32.4 ± 1.6	23.3 ± 1.6	~12.6	26.5 ± 1.4
m4	–	–	–	~49.5	33.1 ± 1.5	17.7 ± 5.1	11.4 ± 2.5
m5	–	–	–	–	–	–	21.2 ± 3.3
m6	–	–	~9.8	–	–	27.7 ± 6.7	11.8 ± 1.2
m7	–	–	~11.4	–	–	–	12.0 ± 1.7
m8	–	–	–	–	~48.2	41.5 ± 7.8	16.4 ± 1.1
m9	–	–	–	–	42.4 ± 7.3	36.6 ± 7.4	21.5 ± 1.6
m10	–	–	–	–	6.9 ± 4.8	6.9 ± 2.7	3.5 ± 0.9
m11	–	–	–	24.3 ± 3.8	15.9 ± 3.4	14.4 ± 4.6	8.4 ± 0.2
m12	–	–	–	–	–	~51.9	–
m13	–	–	~50.1	–	–	–	–
m14	–	–	~43.1	–	–	–	31.8 ± 0.7
AG-1295	–	–	9.9 ± 1.9	–	–	–	7.7 ± 0.9
Monepantel	0.5 ± 0.2	0.3 ± 0.1	0.2 ± 0.1	0.8 ± 0.3	0.3 ± 0.2	0.4 ± 0.3	0.07 ± 0.04

'~' indicates where half maximum inhibitory concentration could not be accurately calculated by the log (inhibitor) versus response - variable slope (four parameter) equation and IC_{50} value was estimated; '–' = no activity.

In the test for inhibition of L4 development after 7 days of incubation, all compounds (except those that were less potent: m2, m12 and m13) demonstrated IC_{50} values ranging from 3.5 ± 0.9 μM to 31.8 ± 0.7 μM (Table 1; Fig. 2C). Like in the L4 motility assay, compound m10 was also most effective at inhibiting L4 development, with an IC_{50} value of 3.5 ± 0.9 μM.

Overall, these findings revealed that different members of this chemical series are able to inhibit xL3 motility, L4 motility and L4 development with potencies in the tens of μM; compound m10 was most potent at inhibiting the development from xL3 to L4 and the motility of the L4 stage (Table 1; Fig. 2).

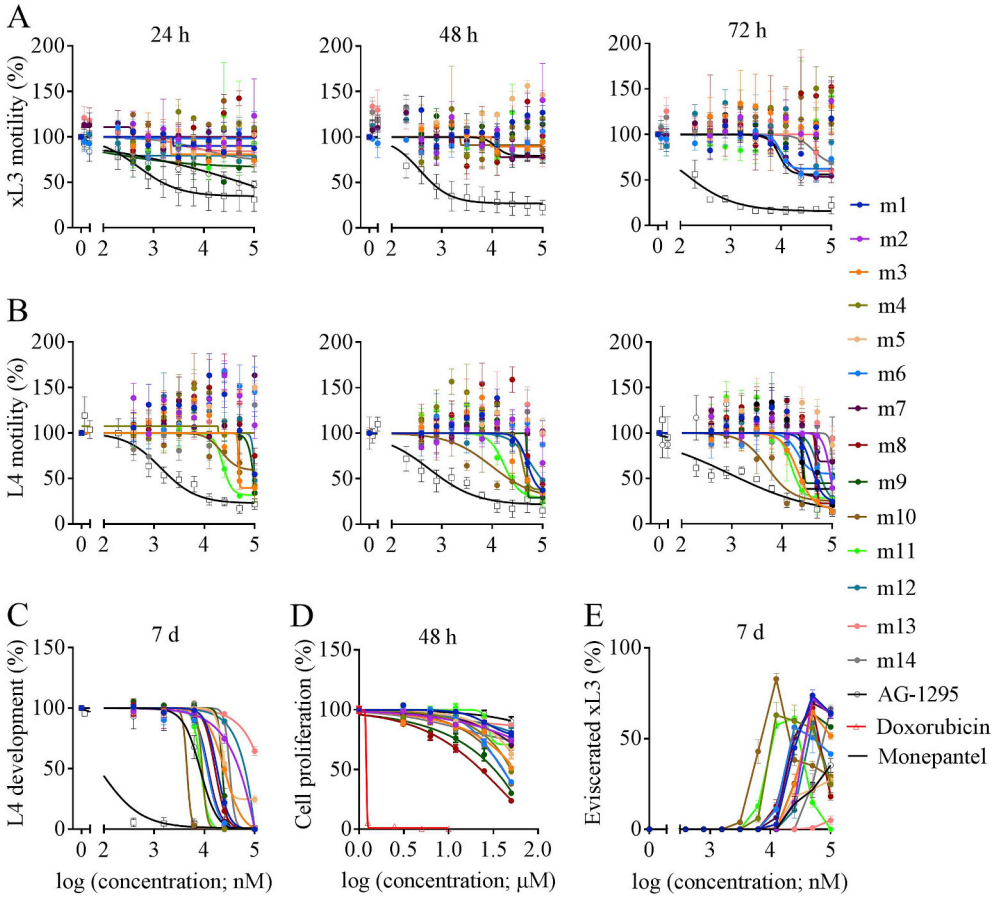

Fig. 2. Dose-response curves of the effects of 14 AG-1295 analogues against *Haemonchus contortus* in vitro. Panel A: Inhibition of the motility of exsheathed third-stage larvae (xL3s) at 24 h, 48 h and 72 h. Panel B: Inhibition of the motility of fourth-stage larvae (L4s) at 24 h, 48 h and 72 h. Panel C: Inhibition of the development of L4 development after 7 days. AG-1295 was used as a reference compound. Panel D: Inhibition of the proliferation of normal human breast epithelial (MCF10A) cells; doxorubicin was used as the reference positive-control. Panel E: Commencement of evisceration in xL3s (%) after 7 days. Data points represent at least two independent experiments conducted in triplicate, presented as the mean ± standard error of the mean.

Table 2
In vitro cytotoxicity of tetrahydroquinoxaline compounds against human breast epithelial cells (MCF10A). Comparison of 14 tetrahydroquinoxalines with AG-1295 and doxorubicin (reference and positive-control compounds) for inhibition of MCF10A cell proliferation in vitro (± standard error of the mean). Selectivity indices of these compounds on the motility of fourth-stage larvae (L4s; at 72 h) and development of L4s (at 7 days) were calculated using the formula: Si = IC_{50} for MCF10A cell/IC_{50} for *H. contortus*. Each assay was repeated two times in quadruplicate on different days.

Compound	Cell density (%) at 50 μM	IC_{50} (μM) for MCF10A cells	Selectivity index (SI) for *H. contortus*	
			L4 motility	L4 development
m1	79.6 ± 2.2	> 50	> 1.5	> 2.8
m2	75.7 ± 2.9	> 50	> 0.6	nd
m3	51.3 ± 1.6	> 50	> 4.0	> 1.9
m4	48.2 ± 1.1	> 50	> 2.8	> 4.4
m5	62.9 ± 3.9	> 50	nd	> 2.4
m6	39.6 ± 1.9	35.7 ± 3.1	1.3	3.0
m7	70.3 ± 3.8	> 50	nd	> 4.2
m8	23.8 ± 1.4	30.9 ± 7.0	0.7	1.9
m9	30.2 ± 1.5	25–50	0.7–1.4	1.2–2.3
m10	38.1 ± 1.1	25–50	2.6–7.3	7.1–14.1
m11	70.8 ± 2.4	> 50	> 3.5	> 5.9
m12	80.7 ± 4.0	> 50	> 0.96	nd
m13	87.2 ± 1.8	> 50	nd	nd
m14	73.9 ± 1.2	> 50	nd	> 1.6
AG-1295	90.2 ± 3.9	> 50	nd	> 6.4
Doxorubicin	0.2 ± 0.03 (at 10 μM)	1.2 ± 0.1	nd	nd

nd = not determined due to a lack of half maximum inhibitory concentration (IC_{50}) values needed to calculate a selectivity index (SI).

3.2. Cytotoxicity of AG-1295 analogues on MCF10A cells

The next step was to estimate the toxicity and selectivity of the 14 AG-1295 analogues on MCF10A cells with reference to doxorubicin - which reduced the final cell density to 0.3 ± 0.03% of the untreated control at the highest concentration tested (10 μM), with an IC_{50} of 1.2 ± 0.1 μM (Table 2). Consistent with results from a previous study (Jiao et al., 2017a), AG-1295 displayed very limited inhibition of MCF10A cell proliferation, resulting in a final cell density of 90.2 ± 3.9% of the control at 50 μM. The cytotoxicity of the analogues in this assay varied markedly, from those which kept cell density to 25% of control to those that allowed it to reach 87% at 50 μM (Table 2; Fig. 2D). Of the 14 test compounds, the four most potent chemicals (m6, m8, m9 and m10) in this assay showed IC_{50} values ranging from 25 μM to 50 μM (Table 2; Fig. 2D). Based on these values, selectivity indices of 0.6–14.1 for the inhibition of L4 motility and L4 development were calculated; thus, compounds m10 and m11 appeared to be the most selective compounds for *H. contortus* in vitro (Table 2).

3.3. Microscopic characterisation of the Evi phenotype in xL3s exposed to test compounds

While assessing the inhibitory effects of individual AG-1295 analogues on xL3 motility, we observed a non-wildtype phenotype in a large percentage of worms exposed to each of the 14 compounds (100 μM, 72 h), in contrast to wildtype xL3s incubated in LB* with 0.5% DMSO (negative control) (Fig. 1C and D). Non-wildtype xL3s failed to moult to L4s, whereas wildtype xL3s in LB* containing 0.5% DMSO developed unhindered to L4s with discernible mouthparts and pharynx (Fig. 1C).

Detailed light microscopic examination (100-times magnification) with phase-contrast optics revealed that the Evi phenotype in xL3s was characterised by a protrusion of the alimentary tract and surrounding tissues through or around the excretory pore (Fig. 3A), while the excretory canal was clearly visible in untreated xL3s in the same area (Supplementary file 2A). An examination of timed video recordings revealed that evisceration was a gradual but relatively rapid process (< 20 min) (Supplementary file 2B). Initially, a few globular structures emerged from the excretory pore (109.5 ± 1.9 μm from the anterior tip of the xL3), followed by an expulsion of the anterior and, sometimes, the posterior part of the intestine, forming an external 'balloon', with ingesta and body fluids flowing to the exterior of the worm (Fig. 3A; Supplementary file 2B). At this later stage, the breach in the body wall seemed to expand, and the eviscerated mass ended up being located about 80–90 μm from the anterior tip of the worm (Fig. 1C; Fig. 3A; Supplementary file 2B). This Evi phenotype was observed exclusively in xL3s (but not in L4s) exposed to any of the 14 compounds.

An SEM study provided a detailed insight into the protrusion of the alimentary tract and surrounding tissues, and into the wrinkled cuticular surface of treated xL3s (Fig. 3B). Although the Evi phenotype was not observed in L4s, detailed SEM examination revealed a shrivelling in the cuticular surface of such larvae, compared with the smooth cuticular surface of untreated L4s (Fig. 3B); xL3s or L4s exposed to LB* containing the corresponding concentration of DMSO (negative control) were unaffected. A TEM examination revealed a release of the hypodermis from the undulated cuticle of treated xL3s, with pathological alterations in internal organs and tissues, including excretory canals, whereas in untreated xL3s the hypodermis was consistently connected to the cuticle, and no anatomical changes were evident (Fig. 3C). The cuticular shrivelling seen in L4s by SEM likely related to the pathological alterations observed by TEM in compound-treated larvae (detached hypodermis; myodegeneration; cell lysis; and the appearance of electron-dense vesicles) (Fig. 3C). Such alterations were not observed in untreated L4s maintained in culture for the same time.

Members of this compound series were also shown to inhibit larval growth. After measuring 30 xL3s treated with 12.5 μM m10 or LB* + 0.5% DMSO for 72 h, it was shown that compound treatment reduced xL3 length from 641 ± 4.6 μm to 456 ± 11.2 μm. Width was similarly reduced from 18 ± 0.2 μm to 16 ± 0.4 μm (Supplementary file 3). Statistical analyses, using a one-way ANOVA with Tukey's test, showed the differences to be significant (Supplementary file 3). Similarly, the lengths and widths of treated L4s (601 ± 9.6 μm and 18 ± 0.3 μm) were reduced with respect to untreated L4s (624 ± 12.2 μm and 21 ± 0.3 μm), with the difference in width being statistically significant ($P < 0.0001$; Supplementary file 3). Thus, members of this compound series suppress larval growth, in addition to inhibiting larval motility and development.

3.4. Determining the optimum compound concentrations to induce the Evi phenotype in xL3s

The percentages of eviscerated xL3s following 7 days of exposure to each of the 14 compounds were assessed using a ten-step, two-fold serial dilution (100 μM–0.4 μM) (Table 3; Fig. 2E). The maximum percentages of such xL3s ranged from 5.0 ± 2.3% to 82.9 ± 3.1%. The most potent compound to induce this phenotype was m10, resulting in evisceration in 82.9 ± 3.1% of xL3s at 12.5 μM. Interestingly, there was an optimum concentration for each inhibitor to induce the Evi phenotype, most clearly seen for m10, but discernible for most compounds; exposure to higher or lower concentrations resulted in lower percentages of eviscerated larvae (Table 3; Fig. 2E).

Efficacy at inducing the Evi phenotype was clearly related to compound inhibitory potency in the larval motility or development assay. As all data sets were normally distributed, according to the D'Agostino-Pearson normality test, the Pearson correlation coefficient (r) was compared between the potencies of individual compounds to induce the Evi phenotype (xL3s) and the IC_{50} values measured either in the L4 motility assay (r = 0.73) or in the L4 development assay (r = 0.80) (Fig. 4; data normalised by defining the maximum percentage of eviscerated xL3s as 100% for each compound). Thus, the more potent a

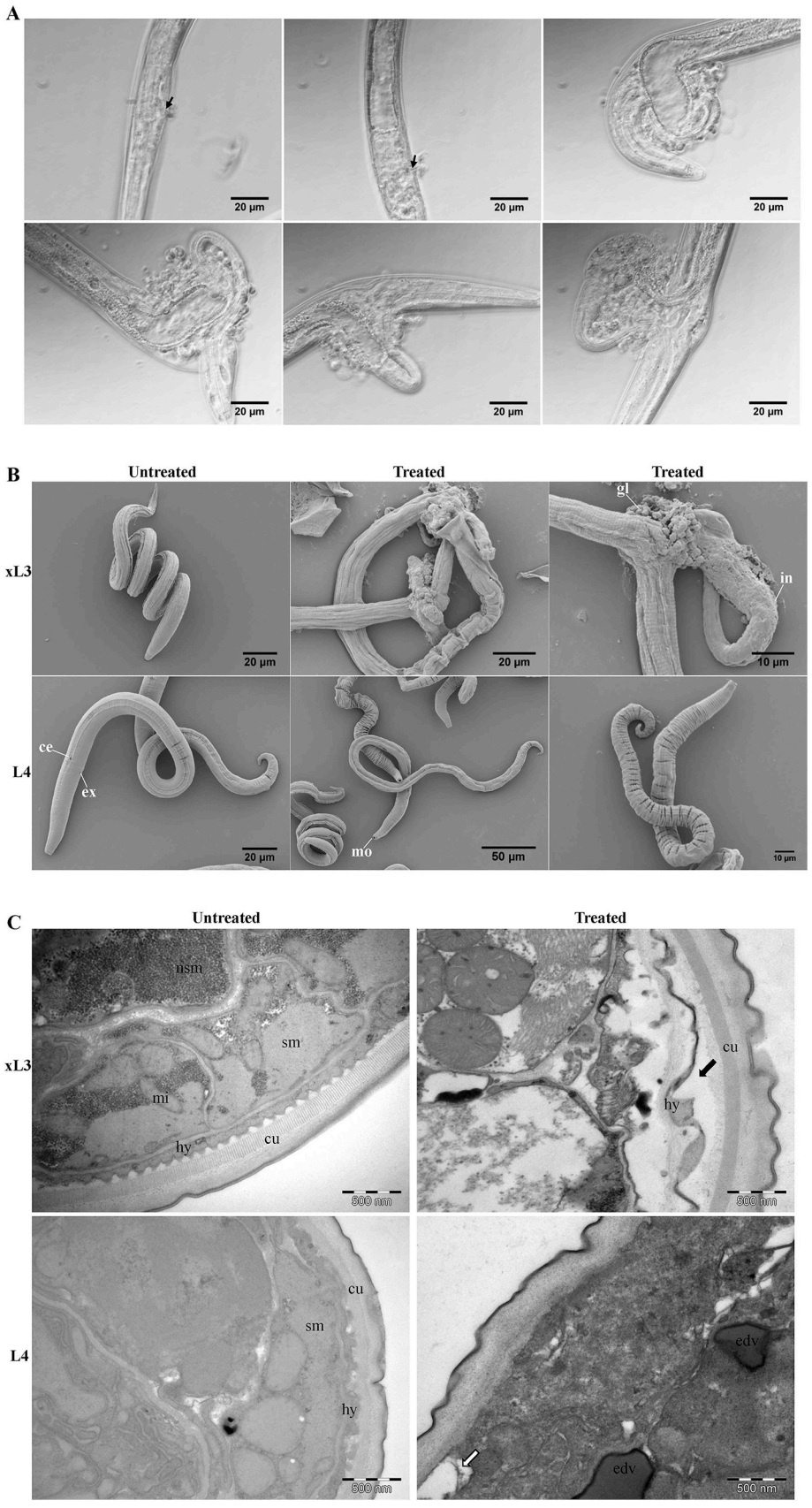

Fig. 3. Microscopy of representative exsheathed third-stage (xL3s) and fourth-stage (L4s) larvae of *Haemonchus contortus*. Panel A: Phase-contrast light microscopy of xL3 following exposure to 12.5 µM of m10. Black arrows indicate excretory canals in xL3. Panel B: Scanning electron microscopy of xL3 (top) and L4 (bottom) stages, following exposure to 12.5 µM of m10 or 0.0625% DMSO (untreated control). Abbreviations: ce = cervical papillae; ex = excretory pore; gl = globules; in = intestine; mo = mouthparts. Panel C: Transmission electron microscopy of xL3 (top) and L4 (bottom) stages following exposure to 12.5 µM of m10 or 0.0625% DMSO (untreated control). A black arrow indicates a release of the hypodermis from the cuticle (appearing undulated) in treated xL3s. A white arrow indicates myo-degeneration and cell lysis in treated L4s. Abbreviations: cu = cuticle; hy = hypodermis; sm = striated muscle; nsm = non-striated muscle; mi = mitochondria; edv = electron-dense vesicles.

Table 3
Frequency of the eviscerated third-stage larvae (xL3s) of *Haemonchus contortus* exposed to individual test compounds (m1 to m14) and the control compound (AG-1295) at different concentrations for 7 days (± standard error of the mean). This assay was repeated two times in triplicate on different days.

Compound	Eviscerated xL3s (%) when exposed to different compound concentrations (μM)										Maximum (%)	Optimum concentration (μM)
	100	50	25	12.5	6.25	3.12	1.56	0.78	0.39	0		
m1	63.9 ± 2.7	73.8 ± 3.2	44.9 ± 3.9	2.8 ± 0.3	0	0	0	0	0	0	73.8 ± 3.2	50
m2	63.3 ± 1.8	72.3 ± 1.1	14.9 ± 1.5	0	0	0	0	0	0	0	72.3 ± 1.1	50
m3	51.5 ± 2.1	64.6 ± 3.6	24.7 ± 5.8	0	0	0	0	0	0	0	64.6 ± 3.6	50
m4	24.9 ± 5.4	55.8 ± 4.5	59.8 ± 8.7	62.9 ± 7.1	6.1 ± 2.0	0	0	0	0	0	62.9 ± 7.1	12.5
m5	21.2 ± 6.0	22.1 ± 2.0	18.0 ± 2.8	1.1 ± 1.1	0	0	0	0	0	0	22.1 ± 2.0	50
m6	41.5 ± 1.4	50.6 ± 8.4	56.3 ± 3.2	11.1 ± 3.6	0	0	0	0	0	0	56.3 ± 3.2	25
m7	64.2 ± 3.2	69.7 ± 3.9	50.6 ± 4.9	6.5 ± 1.2	0	0	0	0	0	0	69.7 ± 3.9	50
m8	18.2 ± 2.1	67.0 ± 2.5	50.5 ± 4.7	12.8 ± 3.4	0	0	0	0	0	0	67.0 ± 2.5	50
m9	56.5 ± 0.4	63.8 ± 4.3	25.2 ± 5.2	0	0	0	0	0	0	0	63.8 ± 4.3	50
m10	29.1 ± 2.1	35.2 ± 2.6	38.3 ± 3.2	82.9 ± 3.1	42.9 ± 6.5	3.9 ± 1.1	0	0	0	0	82.9 ± 3.1	12.5
m11	0	14.8 ± 2.6	61.2 ± 4.5	57.5 ± 2.1	12.9 ± 3.0	0	0	0	0	0	61.2 ± 4.5	25
m12	26.6 ± 3.1	58.4 ± 1.5	10.7 ± 4.5	0	0	0	0	0	0	0	58.4 ± 1.5	50
m13	5.0 ± 2.3	0.8 ± 0.8	0	0	0	0	0	0	0	0	5.0 ± 2.3	100
m14	66.3 ± 2.2	25.1 ± 5.7	0	0	0	0	0	0	0	0	66.3 ± 2.2	100
AG-1295	35.3 ± 3.9	21.8 ± 4.2	14.1 ± 4.0	0	0	0	0	0	0	0	35.3 ± 3.9	100

compound was at inhibiting larval motility or development, the lower the concentration required to eviscerate a maximum number of xL3s.

3.5. Dynamics of evisceration in xL3s

We recorded phenotypic changes in xL3s over time to determine the kinetics of evisceration. Compound m10 was selected for this purpose, as it was the most potent chemical at inhibiting larval motility and development and at inducing evisceration; m7 (a less potent compound) was also selected for comparison with m10. Concentrations of m10 (12.5 μM) and m7 (50 μM) that achieved maximum numbers of eviscerated xL3s at 7 days of exposure were used (Table 3). We measured the percentage of xL3s with an anterior protrusion every 6 h for the first 4 days and then every 24 h for the next three days (Fig. 5). Evisceration was microscopically detected first at 42 h of exposure to compounds m7 and m10. This was the time at which the first L4s were detected in untreated control wells (Fig. 5). The percentage of eviscerated xL3s increased gradually over time, from 3–16% at 42 h to 65–78% at 72 h, and 83–87% at 7 days. From 66 h onwards, the percentages of eviscerated larvae paralleled the number of developed L4s in unexposed control wells (Fig. 5). According to results from a two-way ANOVA with Tukey's test, there were no significant differences between the percentage of eviscerated xL3s after m10 treatment and the percentage of L4s in untreated control wells, except at one time point; there were also no significant differences in the percentage of eviscerated xL3s between m7 and m10 treatments over time, except at three time points (Fig. 5). To increase the time resolution of observations made between 36 h and 48 h, an independent examination of video recordings, taken every 20 min following treatment with m10, showed that the percentages of eviscerated xL3s increased gradually from 42 h onwards (Supplementary file 4), supporting previous observations.

3.6. Reversibility of compound-induced effects and sensitivity time-window

To investigate when the critical process inhibited by the compounds took place during the 7-day development period from xL3 to L4, xL3s were exposed to 12.5 μM of m10 and then washed free of compound at different times and re-incubated in LB* for up to 72 h. Compound was removed after 18 h, 24 h, 27 h, 30 h, 36 h or 48 h of larval treatment, or not at all in the treated control. The percentages of eviscerated xL3s at 72 h were not significantly different from zero when the compound was removed at early time points, up to 36 h. Once larvae had been exposed for at least 36 h, the number of eviscerated larvae began to increase significantly until the end of the experiment (one-way ANOVA with Tukey's test) (Table 4; Fig. 6A). Therefore, the sensitivity window for this particular phenotype opens sometime between 30 h and 36 h. To estimate when it closes, m10 was added to the larvae in culture medium after different times of incubation. When added at 39 h, substantial numbers of eviscerated xL3s were still produced (42.4 ± 3.4%), but compound addition at 42 h had a significantly reduced effect (15.4 ± 2.8% of eviscerated larvae) (Table 4, Fig. 6B). Of note, while most xL3s treated at 42 h were not eviscerated, they were, nevertheless, blocked from developing to L4s (Table 4, Fig. 6B). Thus, the action of m10 blocks xL3 to L4 development, induces pathological changes to the

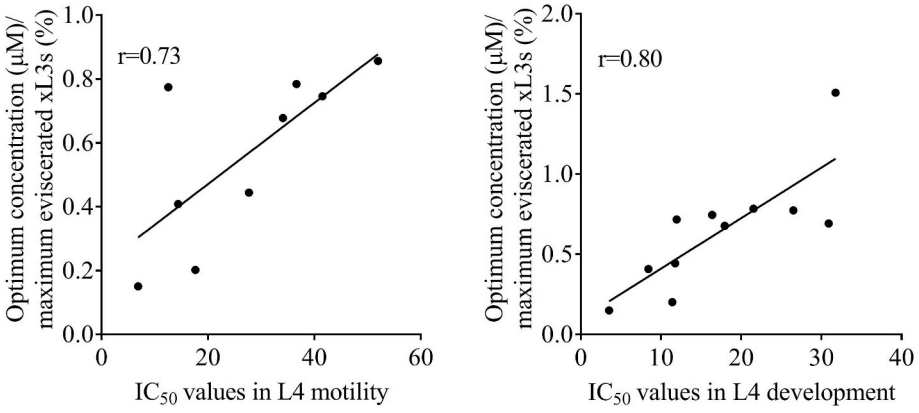

Fig. 4. Pearson correlation coefficients (r) between half maximum inhibitory concentration (IC_{50}) of the motility of fourth-stage larvae (L4s) of *Haemonchus contortus* and the normalised, optimum compound concentration inducing maximum evisceration (%) in the exsheathed third-stage larvae (xL3s) (left panel); Pearson correlation coefficients (r) between IC_{50} of L4 development and the normalised optimum compound concentration inducing maximum evisceration in xL3s (%) (right panel). The optimum compound concentration was normalised by defining the maximum evisceration in xL3s as 100% for individual compounds.

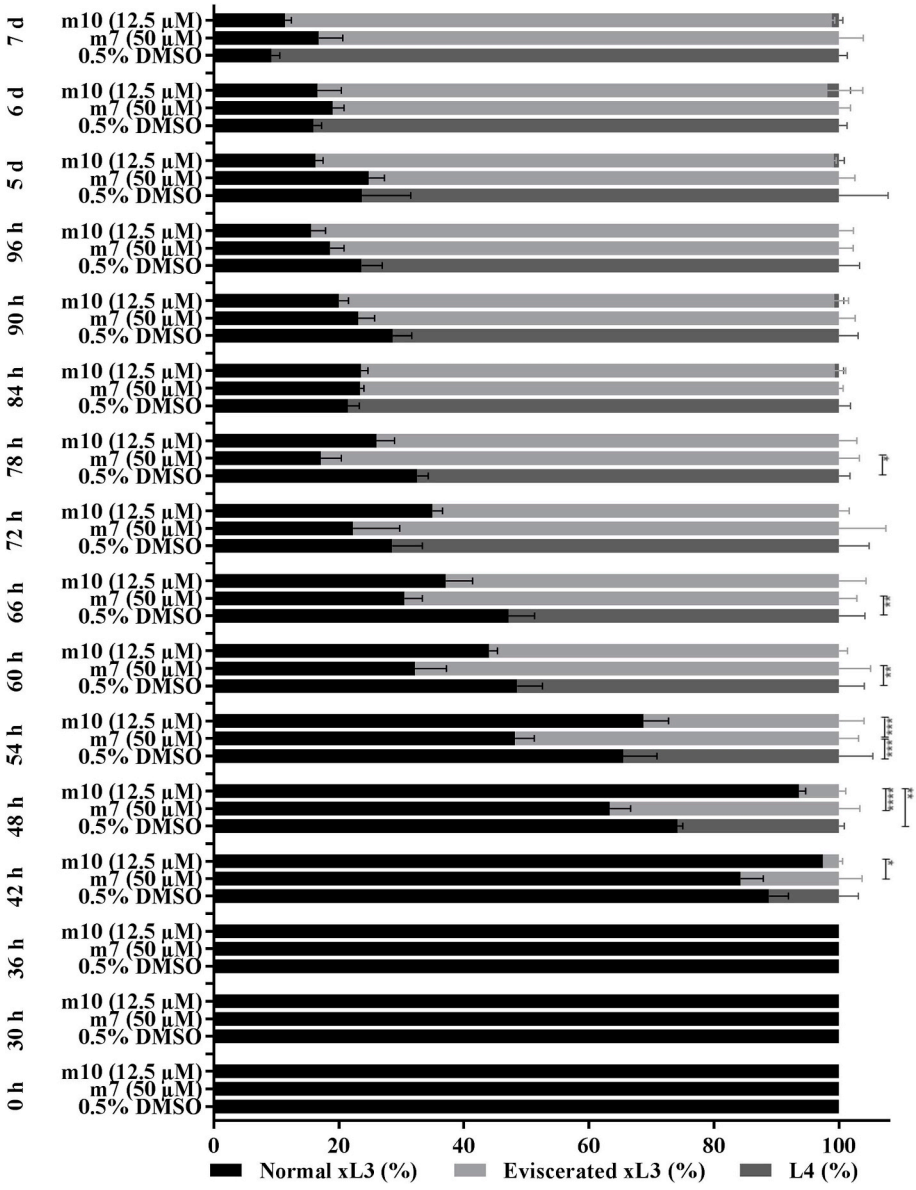

Fig. 5. The dynamics of the compound-induced Evi phenotype in exsheathed third-stage larvae (xL3s) of *Haemonchus contortus*. After exposure to 50 µM of compound m7 or 12.5 µM of compound m10 or only LB* containing 0.5% DMSO (negative-control), the normal xL3s, eviscerated xL3s and fourth-stage larvae (L4s) were examined by light microscopy (20–100 × magnification) at the times indicated on the left. For each time point, the mean percentage of eviscerated larvae in 30 xL3s ± the standard error of the mean was calculated, and a two-way ANOVA with Tukey's test was used to calculate statistical differences between different groups. Asterisks indicate values that are significantly different from one another (*$P < 0.05$; **$P < 0.01$; ***$P < 0.001$; ****$P < 0.0001$). This assay was repeated at least two times in triplicate on different days.

worm (Subsection 3.3) and inhibits motility of the L4 stage. It additionally induces a mechanistically interesting Evi phenotype in xL3s, when added between 30 h and not much later than 42 h, during development of *H. contortus* xL3s to L4s in vitro. This time window seems to coincide with the first appearance of L4s in untreated controls (Fig. 5), suggesting that the Evi phenotype and moulting are linked.

3.7. Influence of external osmotic pressure on the evisceration of xL3s

We reasoned that the most likely driving force behind the dramatic Evi phenotype was an osmotic pressure gradient between the medium and the larval pseudocoelomic fluid, such that it might be possible to protect xL3s to some extent by reducing the pressure differences between the inside and outside of the larvae. To test this hypothesis, xL3s were treated with 12.5 µM m10 in the presence of increasing concentrations of sorbitol (an inert sugar) in LB* (Fig. 7A, left). The osmotic pressure in nematode pseudocoelomic fluid has been reported as 323–400 mOsm/L (Harpur and Popkin, 1965; Fuse et al., 1993; Davey, 1995), and it is 240 mOsm/L in LB (Rothe et al., 2012); antimicrobials in LB* add less than 1 mOsm/L to the medium. Here, it was found that increasing external osmotic pressure with sorbitol indeed protected compound-treated larvae from being eviscerated, commencing at 0.2 M sorbitol in LB* (440 mOsm/L) (Fig. 7A, left). We also observed that sorbitol inhibited untreated larvae from moulting (Fig. 7A, middle), an osmotic effect described previously (Sommerville, 1976). Interestingly, protection of treated xL3s from evisceration by sorbitol mirrored the inhibition of moulting in untreated larvae (Fig. 7A, right). This inhibition was reversible; the removal of sorbitol at 48 h led to a recovery of L4 development to ~80%, comparable with the no-sorbitol control at 7 days (Fig. 7B, left). While moulting was inhibited by sorbitol, compound m10 had no effect on xL3 viability (Fig. 7B, left), and the removal of both compound and sorbitol at 48 h led to a resumption of L4 development, with only 7% of larvae eviscerating (Fig. 7B, right). However, in the no-sorbitol control, the removal of m10 at 48 h still induced the Evi phenotype in a large fraction of xL3s, with only a small percentage (~18%) reaching the L4 stage by 7 days (Fig. 7B, right). Collectively, these findings show that compound m10 (at 12.5 µM) did not affect xL3s, unless they entered the moulting process.

Table 4
Reversibility of the inhibitory property of selected tetrahydroquinoxaline, 12.5 μM of m10, on the exsheathed third-stage larvae (xL3s) of *Haemonchus contortus*. The compound was washed off or added at the times indicated on the table, with corresponding concentration of DMSO as negative-control (± standard error of the mean). This assay was repeated two times in duplicate on different days.

Compound washed at	Eviscerated xL3s (%)	
	At time of washing	After 72 h
18 h	0	0
24 h	0	3.1 ± 2.2
27 h	0	3.9 ± 3.9
30 h	0	6.8 ± 2.0
36 h	0	38.1 ± 4.8
48 h	10.7 ± 2.9	52.3 ± 5.5
No wash	na	66.8 ± 3.0
Untreated control	na	0

Compound added at	**Eviscerated xL3s (%) at 72 h**	**L4 development (%) at 72 h**
0 h	65.0 ± 1.6	0
39 h	42.4 ± 3.4	11.9 ± 1.3
42 h	15.4 ± 2.8	13.4 ± 1.1
Untreated control	0	58.7 ± 2.6

na = not applicable.

4. Discussion

Extending a study (Jiao et al., 2017a) that identified a quinoxaline compound, AG-1295, as being inhibitory to *H. contortus* motility, we sought to investigate whether the anthelmintic activity of AG-1295 was a unique occurrence to this particular compound or a property of the quinoxaline chemical series that could be chemically modulated. The results of the present investigation show that AG-1295 is not a singleton and that a series of 14 analogues have varying degrees of activity, paving the way to structure-activity relationships through future chemical optimisation. We recorded marked inhibitory effects of individual test compounds on larval motility or development and a striking Evi phenotype in xL3s in vitro.

In the primary screen, these compounds were identified as 'hits' based on their induction of a unique larval phenotype and their ability to inhibit L4 development, unlike in previous screens, in which 'hit' compounds were identified by a ≥70% reduction in xL3 motility (Preston et al., 2015). Subsequent compound evaluation confirmed a relatively limited potency of these compounds at inhibiting xL3 motility, with only four of them achieving IC_{50} values in the range of 10 μM–50 μM. These findings indicated that other complementary endpoints, such as morphological phenotype, in addition to xL3 motility, could be employed to refine the detection of 'hits' through in vitro screening.

Most (n = 11) of the test compounds were shown to be more potent

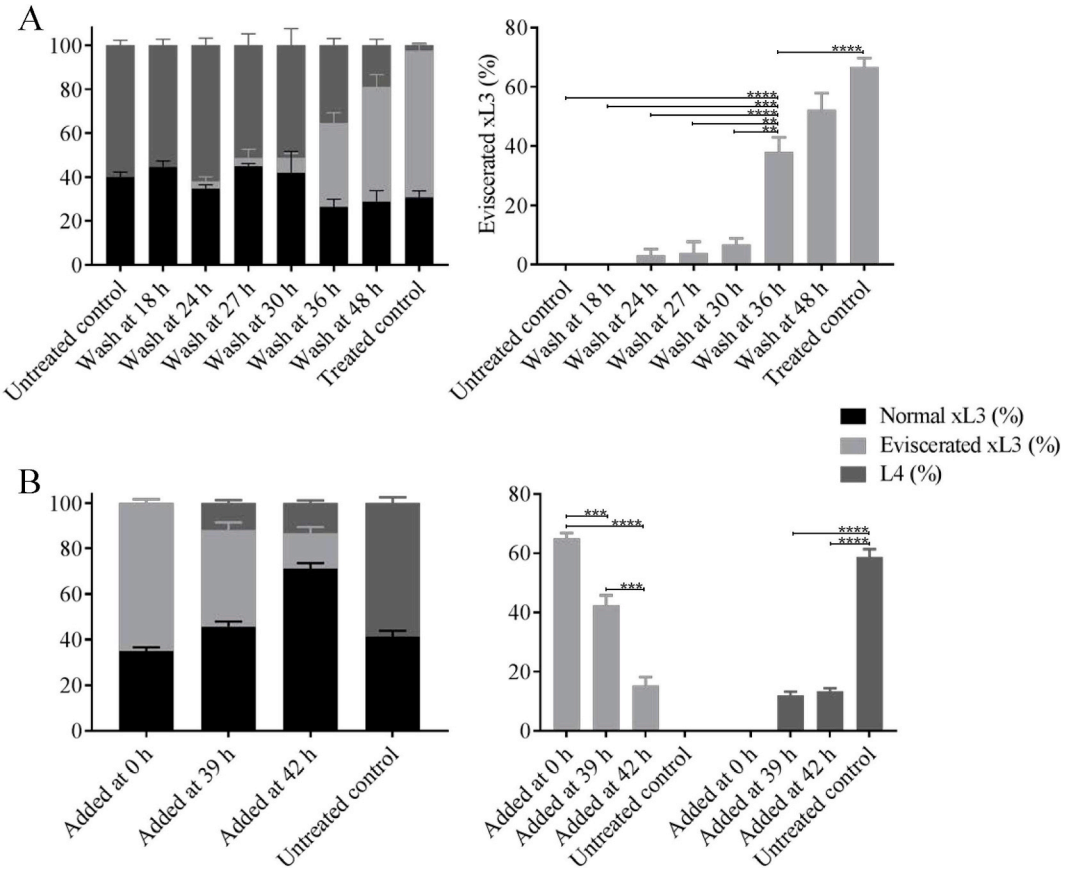

Fig. 6. Reversibility of the effect of individual AG-1295 analogues on the exsheathed third-stage larvae (xL3s) of *Haemonchus contortus*. Panel A: At different time points (18 h, 24 h, 27 h, 30 h, 36 h and 48 h following compound treatment), test compounds (12.5 μM of m10) were removed by washing from wells. At 72 h of exposure, the percentage of xL3s with an Evi phenotype and the rate of development of fourth-stage larvae (L4s) were assessed (left). The controls included xL3s continually exposed to 12.5 μM of individual test compounds for 72 h (treated control) and xL3s incubated in LB* alone (untreated control). A one-way ANOVA with Tukey's test was used to calculate statistical differences in the percentage of eviscerated xL3s between treatments (right). Panel B: Compounds were added at 39 h and 42 h after first culturing larvae; the percentage of xL3s with an Evi phenotype and rate of L4 development were assessed at 72 h. A two-way ANOVA with Tukey's test was used to calculate statistical differences between groups. This assay was repeated two times in duplicate on different days. Asterisks indicate values (mean ± the standard error of the mean) that are significantly different from one another (**$P < 0.01$; ***$P < 0.001$; ****$P < 0.0001$).

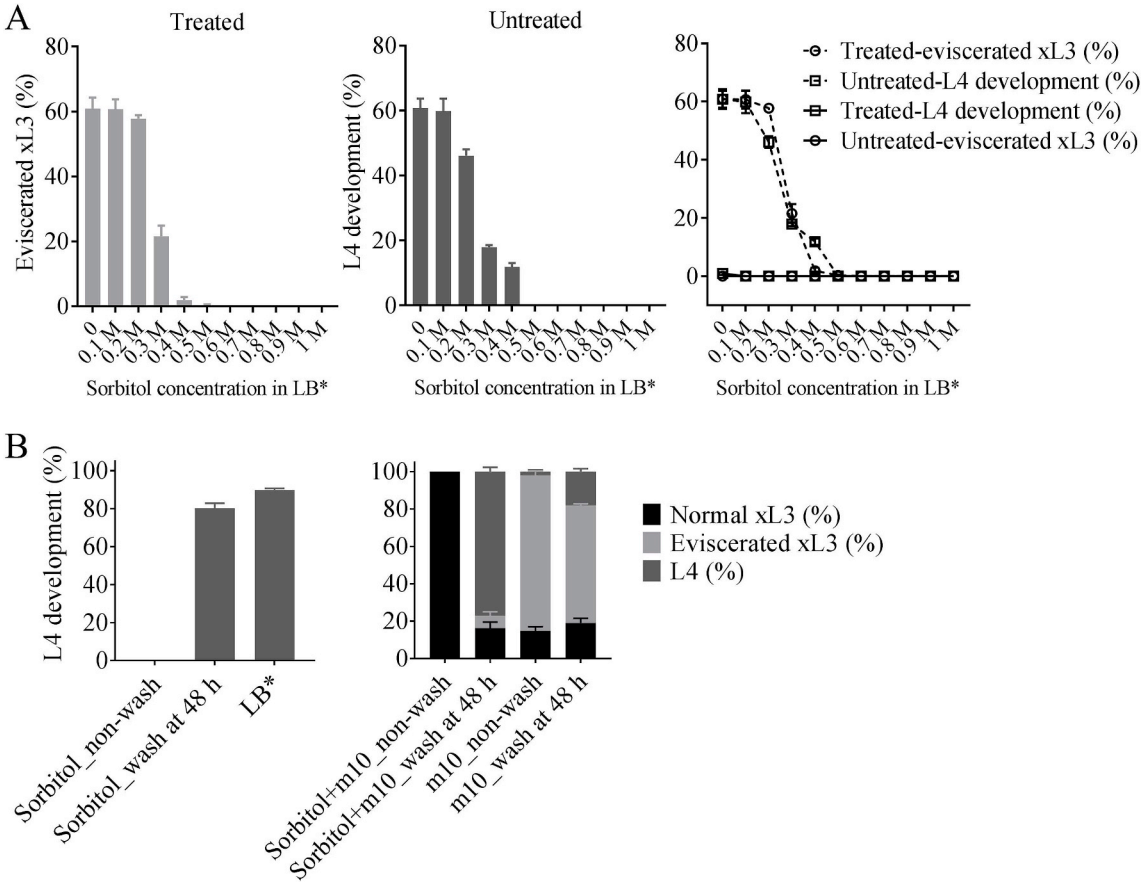

Fig. 7. Effect of external osmotic pressure on the compound-induced Evi phenotype in exsheathed third-stage larvae (xL3s) of *Haemonchus contortus*. Compound m10 was used to treat xL3s at the concentration of 12.5 μM. Panel A: Compound-treated xL3s (left) and untreated xL3s (middle) were cultured in the presence of increasing concentrations of sorbitol in LB*, as indicated in the figure. At 72 h, the percentage of xL3s with an Evi phenotype and the rate of development of fourth-stage larvae (L4s) were evaluated. Increased osmotic pressure in the culture medium reduced evisceration in treated xL3s (%), mirroring the inhibition of moulting in untreated xL3s (right). Panel B: xL3s cultured in the presence of 0.6 M of sorbitol were washed at 48 h, and the rate of L4 development was counted at 7 days to test the reversibility of sorbitol in inhibiting xL3 moulting (left); the controls included xL3s continually incubated in 0.6 M of sorbitol for 7 days, and xL3s incubated in LB* alone for the same time period; xL3s exposed to 12.5 μM of m10 in the presence of 0.6 M of sorbitol were washed at 48 h and examined microscopically after 7 days, to test the effect of test compound on xL3s when xL3 moulting was inhibited (right); the controls included unwashed xL3s exposed to 12.5 μM of compound m10 in the presence of 0.6 M of sorbitol, and xL3s exposed to 12.5 μM of m10 in LB*. This assay was repeated two times in duplicate on different days. Each value represents the mean ± standard error of the mean.

at inhibiting the motility of L4s than xL3s (Table 1). Differences in compound penetration, target expression level, metabolism, detoxification and/or efflux (cf. Gill et al., 1991; George et al., 2017) between xL3s and L4s might explain the different potencies of these compounds between these two larval stages. Importantly, L4s possess a pronounced mouth and functional pharynx (for blood feeding in vivo) which likely facilitate drug uptake. Nonetheless, three select compounds (m7, m13 and m14) as well as AG-1295 itself all reduced xL3 motility, but not L4 motility. To fully understand the reasons for varying potencies, a study of structure-activity relationships by chemical modification and drug target identification should be undertaken in this or model nematodes.

Cytotoxicity was tested against a human, non-malignant mammary epithelial cell line (MCF10A), and different members of this series exhibited varied, generally low cytotoxicities (Table 2). Furthermore, there was no correlation between the potency against *H. contortus* and the cytotoxicity against MCF10A cells (Tables 1 and 2). Although the present selectivity (0.6–14.1) is lower than desired, variation among the different compounds indicates that selectivity can be chemically modulated during lead optimisation. In later stages, in vivo toxicity should be investigated to establish the relationship between in vitro and in vivo systems, as they may not correlate perfectly (cf. McKim, 2010; Sayes, 2014).

The initial screening hit and parent compound, AG-1295, has been described as a receptor tyrosine kinase inhibitor (Kovalenko et al., 1994, 1997; Gazit et al., 1996). Whether this is also the mode of anthelmintic action needs to be investigated, but here we conducted a detailed morphological analysis of the effects of the most potent analogue, m10, against xL3s and L4s, using light and electron microscopy. At the relatively low concentration of 12.5 μM, the m10 analogue was observed to cause widespread morphological damage in both larval stages (Fig. 3; Supplementary file 2), but treated xL3s, in particular, suffered from a lethal process (i.e. evisceration), by which an initial small protrusion, located at the level of the excretory pore, rapidly progressed to an extrusion of the intestinal tube plus other pseudocoelomic components (Fig. 3A). Interestingly, all analogues were able to induce this phenotype at an optimum concentration, related to their potency in the anthelmintic assays (Table 3; Fig. 2E; Fig. 4), suggesting that the inhibition of larval motility or development and the induction of the Evi phenotype all result from an inhibition of the same target(s) in *H. contortus*. Nevertheless, while the degree of inhibition of motility or development increased monotonically with compound concentration, the Evi phenotype became less pronounced above an optimum concentration, indicating that some physiological processes have to be disrupted, but not fully inhibited, for evisceration to take place. This

supports a mode of action involving alterations in signalling mechanisms, in agreement with the described activity of AG-1295 and the multiple protein kinases involved in nematode moulting (see Lazetic and Fay, 2017). Another explanation could be compound insolubility above a particular concentration, but this would have also reduced the inhibition of motility or development at the highest concentrations tested, and it did not (Fig. 2A and B).

We also found that there was a particular time window in which the Evi phenotype could be induced in xL3s. Larvae exposed to test compounds for the first 30 h of culture only, before ecdysis started, or to compound added after 42 h, once the first L4s appeared, did not show eviscerations. However, while early treatment, followed by compound removal, did not seem to affect larvae, worms treated after 42 h in culture appeared as morphologically damaged xL3s and L4s. One possible interpretation is that test compounds can only gain access to the larvae once ecdysis starts and the cuticle sloughs, and the morphogenetic process that makes larvae vulnerable to evisceration occurs in a time window of 30 h to 42 h of in vitro culture. An alternative explanation might be that the target for this chemical series is essential only after the beginning of ecdysis. We found that xL3s do survive compound exposure when placed in hypertonic medium (Fig. 7), but we also found that, as previously published (Sommerville, 1976), hypertonic media prevent larval moulting, so it is still unclear whether the target first appears in L4s, or whether it is always present, but the compounds only access the larval interior after ecdysis commences. In support of this latter hypothesis, AG-1295 and analogues m6, m7, m13 and m14 seem able to affect xL3 motility after prolonged exposure (72 h) (Table 1); this might also explain why the kinetics of emergence of the Evi phenotype in xL3s parallel those of moulting (Subsection 3.5).

From a fundamental biological perspective, it would be significant to elucidate the signalling mechanism required to produce the intestinal prolapse through the excretory pore. Supplementary file 2 shows intestinal content moving but being diverted to the pore, not to the mouth or the anus, as if, at this stage, these two openings would not allow passage of material. Clearly, morphogenetic processes are being disrupted, with catastrophic consequences for the worm, indicating that the compounds will have nematocidal activity against larval stages, although activity against adult worms needs to be assessed.

In conclusion, we have established the in vitro anthelmintic activity of this tetrahydroquinoxaline chemical series, a family of compounds derived from a protein tyrosine kinase inhibitor, AG-1295, a known inhibitor of PDGF receptor kinase in humans (Kovalenko et al., 1994, 1997; Gazit et al., 1996). This tyrosine kinase might have been of interest as a drug target in this nematode, but the PDGF receptor kinase family had not been identified in *H. contortus* (Stroehlein et al., 2015; Jiao et al., 2017a). However, other related tyrosine kinase families may serve as a target for the quinoxalines and, thus, have potential as anthelmintic drug targets. If this turns out to be the case, a useful anthelmintic could be developed with a totally novel mode of action, and its further development would benefit from the wealth of knowledge accumulated for compounds targeting protein kinases.

Acknowledgements

The present study was funded by the Australian Research Council (ARC) and the National Health and Medical Research Council of Australia (NHMRC). We thank our colleagues at Medicines for Malaria Ventures (MMV), Faculty of Veterinary and Agricultural Sciences (FVAS) of The University of Melbourne and Monash Institute of Pharmaceutical Sciences (MIPS), in particular Dr Anson Koehler, Dr Tao Wang and Ms Thuy Le, for their support. We also thank A/Prof Kaylene J. Simpson and Ms Karla J. Cowley, Victorian Centre for Functional Genomics, Peter MacCallum Cancer Centre, Parkville, Victoria, for cytotoxicity testing - this Centre is supported by funding from the Australian Government's Education Investment Fund through the Super Science Initiative and the Peter MacCallum Cancer Centre Foundation (KJS). YJ is the grateful recipient of scholarships from the Chinese Scholarships Council (CSC) and The University of Melbourne. The authors declare no conflicts of interest.

Appendix A. Supplementary data

Supplementary data to this article can be found online at https://doi.org/10.1016/j.ijpddr.2018.12.007.

References

Banai, S., Wolf, Y., Golomb, G., Pearle, A., Waltenberger, J., Fishbein, I., Schneider, A., Gazit, A., Perez, L., Huber, R., Lazarovichi, G., Rabinovich, L., Levitzki, A., Gertz, S.D., 1998. PDGF-receptor tyrosine kinase blocker AG1295 selectively attenuates smooth muscle cell growth in vitro and reduces neointimal formation after balloon angioplasty in swine. Circulation 97, 1960–1969.

Beveridge, I., Emery, D., 2014. Australian Animal Parasites - Inside and Out. The Australian Society for Parasitology Inc., Australia ISBN: 978-0-646-93560-7.

Davey, K.G., 1995. Water, water compartments and water regulation in some nematodes parasitic in vertebrates. J. Nematol. 27, 433–440.

Fuse, M., Davey, K.G., Sommerville, R.I., 1993. Osmoregulation in the parasitic nematode *Pseudoterranova decipiens*. J. Exp. Biol. 175, 127–142.

Gazit, A., App, H., McMahon, G., Chen, J., Levitzki, A., Bohmer, F.D., 1996. Tyrphostins. 5. Potent inhibitors of platelet-derived growth factor receptor tyrosine kinase: structure-activity relationships in quinoxalines, quinolines, and indole tyrphostins. J. Med. Chem. 39, 2170–2177.

George, M.M., Lopez-Soberal, L., Storey, B.E., Howell, S.B., Kaplan, R.M., 2017. Motility in the L3 stage is a poor phenotype for detecting and measuring resistance to avermectin/milbemycin drugs in gastrointestinal nematodes of livestock. Int. J. Parasitol. Drugs Drug Resist. 8, 22–30.

Gill, J.H., Redwin, J.M., van Wyk, J.A., Lacey, E., 1991. Detection of resistance to ivermectin in *Haemonchus contortus*. Int. J. Parasitol. 21, 771–776.

Harpur, R.P., Popkin, J.S., 1965. Osmolality of blood and intestinal contents in the pig, Guinea pig, and *Ascaris lumbricoides*. Can. J. Biochem. 43, 1157–1169.

Hewitson, J.P., Maizels, R.M., 2014. Vaccination against helminth parasite infections. Expert Rev. Vaccines 13, 473–487.

Hotez, P.J., Alvarado, M., Basáñez, M.G., Bolliger, I., Bourne, R., Boussinesq, M., Brooker, S.J., Brown, A.S., Buckle, G., Budke, C.M., Carabin, H., Coffeng, L.E., Fèvre, E.M., Fürst, T., Halasa, Y.A., Jasrasaria, R., Johns, N.E., Keiser, J., King, C.H., Lozano, R., Murdoch, M.E., O'Hanlon, S., Pion, S.D.S., Pullan, R.L., Ramaiah, K.D., Roberts, T., Shepard, D.S., Smith, J.L., Stolk, W.A., Undurraga, E.A., Utzinger, J., Wang, M., Murray, C.J.L., Naghavi, M., 2014. The global burden of disease study 2010: interpretation and implications for the neglected tropical diseases. PLoS Negl. Trop. Dis. 8, e2865.

Iwamoto, H., Nakamuta, M., Tada, S., Sugimoto, R., Enjoji, M., Nawata, H., 2000. Platelet-derived growth factor receptor tyrosine kinase inhibitor AG1295 attenuates rat hepatic stellate cell growth. J. Lab. Clin. Med. 135, 406–412.

Jiao, Y., Preston, S., Koehler, A.V., Stroehlein, A.J., Chang, B.C.H., Simpson, K.J., Cowley, K.J., Palmer, M.J., Laleu, B., Wells, T.N.C., Jabbar, A., Gasser, R.B., 2017a. Screening of the 'Stasis Box' identifies two kinase inhibitors under pharmaceutical development with activity against *Haemonchus contortus*. Parasit. Vectors 10, 323.

Jiao, Y., Preston, S., Song, H., Jabbar, A., Liu, Y., Baell, J., Hofmann, A., Hutchinson, D., Wang, T., Koehler, A.V., Fisher, G.M., Andrews, K.T., Laleu, B., Palmer, M.J., Burrows, J.N., Wells, T.N.C., Wang, Q., Gasser, R.B., 2017b. Assessing the anthelmintic activity of pyrazole-5-carboxamide derivatives against *Haemonchus contortus*. Parasit. Vectors 10, 272.

Kaminsky, R., Gauvry, N., Schorderet Weber, S., Skripsky, T., Bouvier, J., Wenger, A., Schroeder, F., Desaules, Y., Hotz, R., Goebel, T., Hosking, B.C., Pautrat, F., Wieland-Berghausen, S., Ducray, P., 2008. Identification of the amino-acetonitrile derivative monepantel (AAD 1566) as a new anthelmintic drug development candidate. Parasitol. Res. 103, 931–939.

Karck, M., Meliss, R., Hestermann, M., Mengel, M., Pethig, K., Levitzki, A., Banai, S., Golomb, G., Fishbein, I., Chorny, M., Haverich, A., 2002. Inhibition of aortic allograft vasculopathy by local delivery of platelet-derived growth factor receptor tyrosine-kinase blocker AG-1295. Transplantation 74, 1335–1341.

Kotze, A.C., Prichard, R.K., 2016. Anthelmintic resistance in *Haemonchus contortus*: history, mechanisms and diagnosis. Adv. Parasitol. 93, 397–428.

Kovacs, A.L., 2015. The application of traditional transmission electron microscopy for autophagy research in *Caenorhabditis elegans*. Biophys. Rep. 1, 99–105.

Kovalenko, M., Gazit, A., Bohmer, A., Rorsman, C., Ronnstrand, L., Heldin, C.H., Waltenberger, J., Bohmer, F.D., Levitzki, A., 1994. Selective platelet-derived growth factor receptor kinase blockers reverse sis-transformation. Cancer Res. 54, 6106–6114.

Kovalenko, M., Ronnstrand, L., Heldin, C.H., Loubtchenkov, M., Gazit, A., Levitzki, A., Bohmer, F.D., 1997. Phosphorylation site-specific inhibition of platelet-derived growth factor beta-receptor autophosphorylation by the receptor blocking tyrphostin AG1296. Biochemistry 36, 6260–6269.

Kumarasingha, R., Preston, S., Yeo, T.C., Lim, D.S., Tu, C.L., Palombo, E.A., Shaw, J.M., Gasser, R.B., Boag, P.R., 2016. Anthelmintic activity of selected ethno-medicinal plant extracts on parasitic stages of *Haemonchus contortus*. Parasit. Vectors 9, 187.

Lane, J., Jubb, T., Shephard, R., Webb-Ware, J., Fordyce, G., 2015. MLA Final Report:

Priority List of Endemic Diseases for the Red Meat Industries. Meat & Livestock Australia Limited (MLA), pp. 209–219 ISBN: 9781741918946.
Lazetic, V., Fay, D.S., 2017. Molting in *C. elegans*. Worm 6, e1330246.
Levitzki, A., 2001. Protein tyrosine kinase inhibitors as therapeutic agents. In: Waldmann, H. (Ed.), Bioorganic Chemistry of Biological Signal Transduction. Springer, Berlin and Heidelberg, pp. 1–15 ISBN: 978-3-662-14697-2.
Levitzki, A., 2010. Chapter 65: protein kinase inhibitors. In: Bradshaw, R.A., Dennis, E.A. (Eds.), Handbook of Cell Signaling, second ed. Elsevier, Amsterdam and Boston, pp. 481–490 ISBN: 978-0-12-374145-5.
Levitzki, A., 2013. Tyrosine kinase inhibitors: views of selectivity, sensitivity, and clinical performance. Annu. Rev. Pharmacol. Toxicol. 53, 161–185.
Little, P.R., Hodge, A., Maeder, S.J., Wirtherle, N.C., Nicholas, D.R., Cox, G.G., Conder, G.A., 2011. Efficacy of a combined oral formulation of derquantel–abamectin against the adult and larval stages of nematodes in sheep, including anthelmintic-resistant strains. Vet. Parasitol. 181, 180–193.
McKim Jr., J.M., 2010. Building a tiered approach to in vitro predictive toxicity screening: a focus on assays with in vivo relevance. Comb. Chem. High Throughput Screen. 13, 188–206.
Preston, S., Jabbar, A., Nowell, C., Joachim, A., Ruttkowski, B., Baell, J., Cardno, T., Korhonen, P.K., Piedrafita, D., Ansell, B.R., Jex, A.R., Hofmann, A., Gasser, R.B., 2015. Low cost whole-organism screening of compounds for anthelmintic activity. Int. J. Parasitol. 45, 333–343.
Preston, S., Jabbar, A., Nowell, C., Joachim, A., Ruttkowski, B., Cardno, T., Hofmann, A., Gasser, R.B., 2016a. Practical and low cost whole-organism motility assay: a step-by-step protocol. Mol. Cell. Probes 30, 13–17.
Preston, S., Jiao, Y., Baell, J.B., Keiser, J., Crawford, S., Koehler, A.V., Wang, T., Simpson, M.M., Kaplan, R.M., Cowley, K.J., Simpson, K.J., Hofmann, A., Jabbar, A., Gasser, R.B., 2017. Screening of the 'Open Scaffolds' collection from Compounds Australia identifies a new chemical entity with anthelmintic activities against different developmental stages of the barber's pole worm and other parasitic nematodes. Int. J. Parasitol. Drugs Drug Resist. 7, 286–294.
Preston, S., Jiao, Y., Jabbar, A., McGee, S.L., Laleu, B., Willis, P., Wells, T.N., Gasser, R.B., 2016b. Screening of the 'Pathogen Box' identifies an approved pesticide with major anthelmintic activity against the barber's pole worm. Int. J. Parasitol. Drugs Drug Resist. 6, 329–334.
Prichard, R.K., Geary, T.G., 2008. Drug discovery: fresh hope to can the worms. Nature 452, 157–158.
Roeber, F., Jex, A.R., Gasser, R.B., 2013. Impact of gastrointestinal parasitic nematodes of sheep, and the role of advanced molecular tools for exploring epidemiology and drug resistance - an Australian perspective. Parasit. Vectors 6, 153.
Rothe, M., Alpert, C., Engst, W., Musiol, S., Loh, G., Blaut, M., 2012. Impact of nutritional factors on the proteome of intestinal *Escherichia coli*: induction of OxyR-dependent proteins AhpF and Dps by a lactose-rich diet. Appl. Environ. Microbiol. 78, 3580–3591.
Sayes, C.M., 2014. The relationships among structure, activity, and toxicity of engineered nanoparticles. KONA Powder Part. J. 31, 10–21.
Sommerville, R.I., 1966. The development of *Haemonchus contortus* to the fourth stage in vitro. J. Parasitol. 52.
Sommerville, R.I., 1976. Influence of potassium ion and osomtic pressure on development of *Haemonchus contortus* in vitro. J. Parasitol. 62, 242–246.
Stroehlein, A.J., Young, N.D., Korhonen, P.K., Jabbar, A., Hofmann, A., Sternberg, P.W., Gasser, R.B., 2015. The *Haemonchus contortus* kinome–a resource for fundamental molecular investigations and drug discovery. Parasit. Vectors 8, 623.
Thamsborg, S.M., Nejsum, P., Mejer, H., 2013. Impact of *Ascaris suum* in livestock. In: Holland, C. (Ed.), *Ascaris*: the Neglected Parasite, first ed. Elsevier, Amsterdam and Boston, pp. 363–381 ISBN: 978-0-12-397285-9.
Veglia, F., 1916. The anatomy and life history of *Haemonchus (Strongylus) contortus* (Rud.). J. Comp. Pathol. Ther. 29, 265–277.